Searching for IceCube sub-TeV neutrino counterparts to sub-threshold Gravitational Wave events

(article starts on next page)

Searching for IceCube sub-TeV neutrino counterparts to sub-threshold Gravitational Wave events

The IceCube Collaboration

(a complete list of authors can be found at the end of the proceedings)

E-mail: tista.mukherjee@kit.edu

Since the release of the Gravitational Wave Transient Catalogue GWTC-2.1 by the LIGO-Virgo collaboration, sub-threshold gravitational wave (GW) candidates are publicly available. They are expected to be released in real-time as well, in the upcoming O4 run. Using these GW candidates for multi-messenger studies complement the ongoing efforts to identify neutrino counterparts to GW events. This in turn, allows us to schedule electromagnetic follow-up searches more efficiently. However, the definition and criteria for sub-threshold candidates are pretty flexible. Finding a multi-messenger counterpart via archival studies for these candidates will help to set up strong bounds on the GW parameters which are useful for defining a GW signal as sub-threshold, thereby increasing their significance for scheduling follow-up searches. Here, we present the current status of this ongoing work with the IceCube Neutrino Observatory. We perform a selection of the sub-threshold GW candidates from GWTC-2.1 and conduct an archival search for sub-TeV neutrino counterparts detected by the dense infill array of the IceCube Neutrino Observatory, known as "DeepCore". For this, an Unbinned Maximum Likelihood (UML) method is used. We report the 90% C.L. sensitivities of this sub-TeV neutrino dataset for each selected sub-threshold GW candidate, considering the spatial and temporal correlation between the GW and neutrino events within a 1000 s time window.

Corresponding author: Tista Mukherjee[1][*]

[1] *Institute for Astroparticle Physics, Karlsruhe Institute of Technology, Karlsruhe, Germany*

[*] Presenter

1. Introduction

The IceCube Neutrino Observatory is a cubic-kilometre ice-Cherenkov detector located in the geographical South Pole. It is mainly sensitive to high-energy neutrinos with an energy of more than 100 GeV. However, after the installation of a dense infill array called 'DeepCore', the energy threshold for neutrino detection by IceCube has been lowered by another order of magnitude, making the detector sensitive to sub-TeV neutrinos with energy < 100 GeV as well [1].

IceCube, with all its resources, has been playing an active role, both in real-time and archival follow-ups to the gravitational wave (GW) alerts sent by LIGO-Virgo-KAGRA (LVK) collaboration [2, 3]. These alerts were sent for the confident events observed during their past three observation runs (O1, O2 and O3). By confident events, we mean events with False Alarm Rate (FAR) < 2 yr^{-1} and the probability of astrophysical origin (p_{astro}) > 0.5. The events are currently listed in the three event catalogues released by LVK, known as Gravitational Wave Transient Catalogue (GWTC) - 1, 2 and 3 [4–6]. However, after the release of GWTC-2, GWTC-2.1 was made public with an updated list of confident GW events from the first half of third observational run (O3a) [7]. Another feature which made the GWTC-2.1 unique was the inclusion of 1201 'sub-threshold candidates' detected during O3a. By 'sub-threshold', we mean GW candidates which could not pass the hard threshold of FAR < 2 yr^{-1}, but they passed a low-significance FAR threshold of 2 day^{-1}. Similarly, 1048 sub-threshold events were further added to the GWTC-3 catalogue as well, detected during the second half of the third observational run (O3b).

From IceCube follow-ups to the confident GW events, no neutrino counterpart was detected [2, 8]. However, the sub-threshold GW candidates were only available after the end of O3. So, they can only be followed up via archival studies. In this work, we are interested in doing that using the candidates we are getting from O3a. The main motivation to search for possible neutrino counterparts of sub-threshold GW candidates is to check if they are significant enough to be followed up in real-time. Also, with the help of IceCube, we can significantly improve the source localisation for sub-threshold GW candidates, which would allow the astronomical community to schedule follow-up campaigns more efficiently.

2. The datasets

2.1 GW sub-threshold candidates

All the GW candidates are identified using four different GW analysis pipelines, i.e., GstLAL, MBTA, PyCBC, and PyCBC-high mass [9–12], developed and used by the LVK collaboration to detect compact binary coalescence (CBC). In the event database for GWTC-2.1, all candidates with FAR < 2 day^{-1} ($\sim$ 730 yr^{-1}) were included. This also indicates that the confident events with FAR < 2 yr^{-1} are not separated from the candidates of our interest for this work. So first, we need to filter out these candidates qualifying as confident GW events for which archival searches have already been done using both high- and low-energy IceCube neutrinos [2, 8]. In Figure 1, we have illustrated the procedure, taking the candidates we are getting from GstLAL as an example. Initially, it included 405 candidates with FAR values ranging from 5×10^{-33} to $\sim$ 730 yr^{-1}. After excluding all the events with FAR < 2 yr^{-1}, we are left with 369 sub-threshold candidates. Similar treatment is done to the candidates identified by the other 3 pipelines.
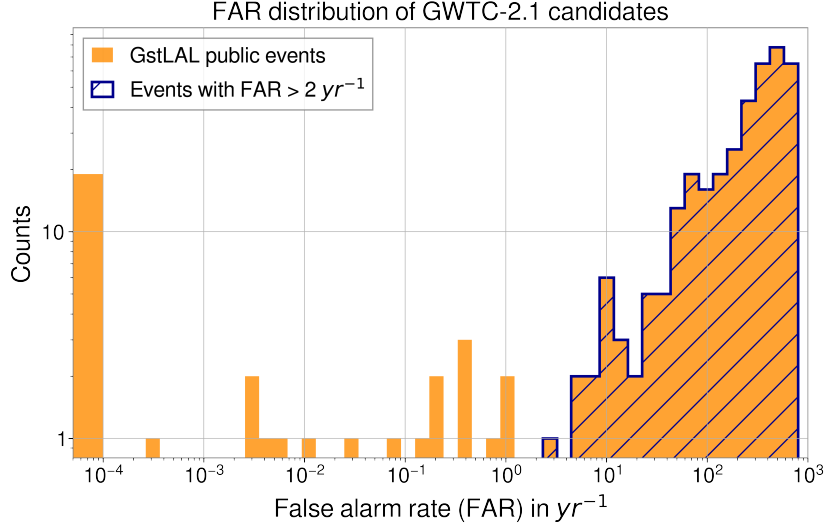
Figure 1: The comparison of the FAR distribution with and without the confident GW events identified by GstLAL during O3a. It is to be noted that the FAR values range from 10^{-33} to 730 yr^{-1} (0 - 2 day^{-1}). The first bin contains all candidates with FAR < 10^{-4} yr^{-1}. After sorting out the confident events, we lose the GW candidates identified by GstLAL with FAR < 2 yr^{-1}. The shaded region represent all sub-threshold candidates with FAR > 2 yr^{-1} from GstLAL. Similar treatment is done for events identified by other three pipelines as well.
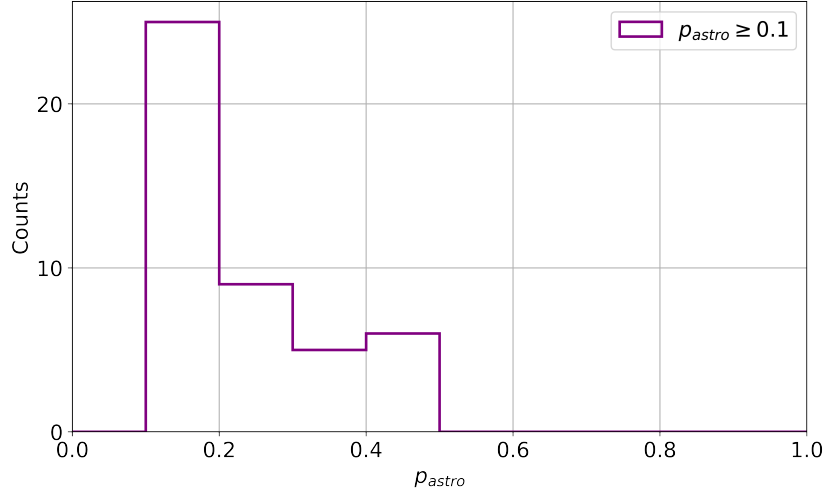
Figure 2: p_{astro} distribution for the 45 sub-threshold GW candidates detected during O3a, to be considered for neutrino counterpart search.

Some of these sub-threshold candidates were later qualified as confident events in the updated GWTC-2.1 catalogue as they had higher p_{astro} or higher SNR or both. We also remove those candidates from our list as they were previously included in the list of GW candidates for archival searches by IceCube. On the leftover candidates, we further impose another filtering criterion of eliminating all the sub-threshold candidates with p_{astro} < 0.1 as they have a higher probability of being terrestrial noise. Some candidates were also double counted by multiple pipelines. In this
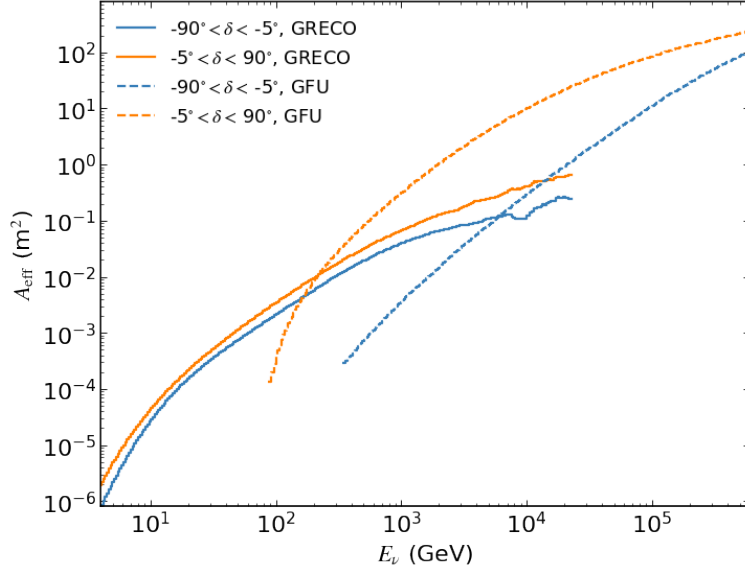
Figure 3: All-flavour effective area for GRECO in different declination bands from [13]. The GFU effective area is shown (dashed line) as reference to compare. It is evident that GRECO has comparable effective area coverage all over the sky, that compliments GFU (sensitive to O(10-100)TeV energy) well in the lower energy range.

case, we only consider the candidate with the highest p_{astro} value from one particular pipeline, at a given event-time. In the end, we are left with 45 unique sub-threshold events which are not included in the updated GWTC-2.1 confident event list. The p_{astro} distribution for these candidates is shown in Figure 2.

2.2 The sub-TeV neutrino dataset (GRECO)

The sub-TeV neutrino dataset available within IceCube is called 'GRECO' (GeV Reconstructed Events with Containment for Oscillations). This is an all-sky, all-flavour dataset, covering the neutrino energy range of O(10-100) GeV. The GRECO events were originally used for neutrino oscillation studies. However, it also has a very stable event rate which makes it suitable for transient searches. It also has a very good effective-area coverage that energy range, evident from Figure 3. It complements the effective area of higher-energy Gamma-ray Follow Up (GFU) events in the energy range of O(10-100) TeV, which is a standard dataset often used to search for astrophysical neutrino transients. For these reasons, the dataset was further optimized for probing transient astrophysical sources from which we can expect sub-TeV neutrinos [14]. Previously, we have used GRECO to search for low-energy neutrino counterparts from the 90 confident GW events from O1, O2 and O3 [8], also from novae [13] and GRBs [15]. In this analysis, it is considered for low-energy neutrino counterpart search to the selected sub-threshold GW candidates from O3a.

3. Analysis Method

To search for the neutrino counterparts, we will follow a Unbinned Maximum Likelihood (UML) analysis. We look for a spatial and temporal coincidence between the selected sub-threshold

GW candidates and GRECO events within a 1000 s (±500 s) time window around the GW event-time. So, in this case, we define two competing hypotheses:

Null hypothesis (H_0): We only have background neutrino events in our data.

Signal hypothesis (H_s): We have injected some signal neutrinos correlated with a specific GW candidate, along with background events.

To test our hypotheses, we define a likelihood function $\mathscr{L}(n_s, \gamma)$, which is given as

$$\mathscr{L}(n_s(\gamma)) = \frac{(n_s + n_b)^N}{N!} e^{-(n_s + n_b)} \prod_{i=1}^{N} \left(\frac{n_s S_i}{n_s + n_b} + \frac{n_b B_i}{n_s + n_b} \right). \tag{1}$$

Here, n_s is and n_b are signal and background neutrino events respectively, where $n_s + n_b = N$, which is the total number of neutrinos. For the signal neutrinos, γ is the spectral index. It is not explicitly shown in the likelihood function '$\mathscr{L}$' because it is implicit in n_s. A Poisson term $e^{-(n_s + n_b)}$ arises to describe the transient nature of the source. S_i and B_i are signal and background probability density for i^{th} event.

We can calculate the likelihood for each hypothesis. Then, we test our H_s where we have some signal neutrinos, n_s which follow a spectrum with spectral index γ, with respect to the background-like H_0. We define the 'Test Statistic' (TS) as

$$TS = max. \left[2 \ln \left(\frac{\mathscr{L}_k(n_s(\gamma)) \cdot \omega_k}{\mathscr{L}_k(n_s = 0)} \right) \right] = TS_{PS} + 2 \ln(\omega_k). \tag{2}$$

As here we are dealing with GW skymaps to search for spatial correlation, we have a spatial prior term ω_k in the numerator of TS, where k is the ID of each pixel in the sky. We divide the GW skymap into 49152 equally-sized pixels. For each pixel, we calculate ω_k as $\frac{(P_{GW})_k}{\Omega_{pixel}}$ where $(P_{GW})_k$ is the probability of having a GW source in the kth pixel. Now for each pixel,

$$2 \ln(\omega_k) = [2 \ln(\omega_k)] - max. [2 \ln(\omega_k)]. \tag{3}$$

So, the maximum value of $2 \ln(\omega_k)$ is 0 for the best-fit GW source location. It is increasingly negative for the pixels where the GW source is less and less likely to be located. Thus, it acts as a spatial penalty term depending on the GW skymap.

4. Analysis Performance

Before starting the analysis, we need to construct the background TS (BGTS) distribution for each sub-threshold GW candidate. This is done by randomly sampling the arrival times of each neutrino event which was detected ± 5 days around the time the GW signal was recorded. This task is repeated 10,000 times, which are designated as individual 'pseudo experiments'. This BGTS distribution is then compared against the TS values we get from an unscrambled neutrino dataset, to search for correlated signal neutrino events. But before doing that, we test the strength of our analysis by 'injecting' signal-like neutrino events from a Monte-Carlo dataset with $\gamma = 2$ on the background-like, scrambled dataset. From this we calculate the 90% sensitivity. This is reported for each selected sub-threshold GW candidate.
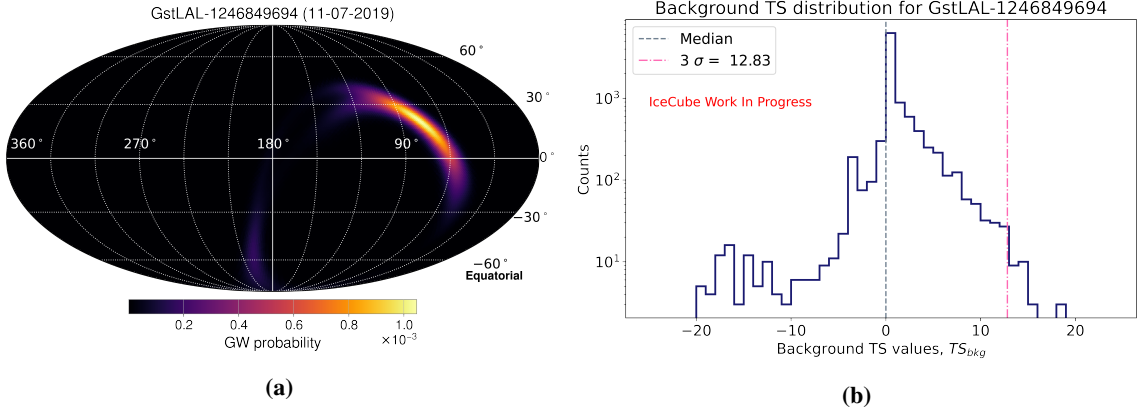
(a)

(b)

Figure 4: Here we consider the sub-threshold GW candidate GstLAL-1246849694 (p_{astro} = 0.35), detected during O3a, as an example. We present (a) the corresponding skymap for this candidate, and (b) the background TS distribution including spatial priors. It contains several negative TS values for the background neutrinos falling on the pixels with highly negative spatial penalty term.

4.1 Background TS distribution

In Figure 4, we present the BGTS distribution we get from one of the sub-threshold GW candidates (GstLAL-1246849694) detected by the LIGO-Virgo-KAGRA collaboration on July 11, 2019, during O3a. The corresponding GW skymap is also shown. One can see that the BGTS distribution contains some dominant spatial features which it gets from ω_k. Most of the BGTS values are negative as most of the background neutrinos fall on the pixels where $2 \ln(\omega_k)$ is highly negative.

4.2 90% Sensitivity flux

The 90% sensitivity is defined as the flux for which the TS value after signal injection is greater than the median of the BGTS distribution for 90% of the trials. We calculate this by injecting
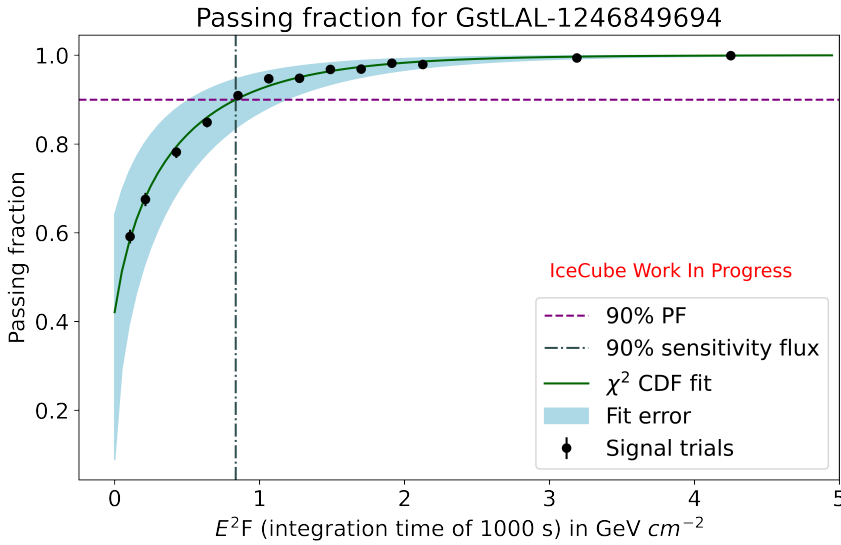

Figure 5: Passing fraction curve for GstLAL-1246849694. The 90% sensitivity flux is pointed out. The time-integrated flux, F (in $GeV^{-1}cm^{-2}$) = $\frac{dN}{dEdAdt} \cdot \delta t$ is computed for δt = 1000 s time window.
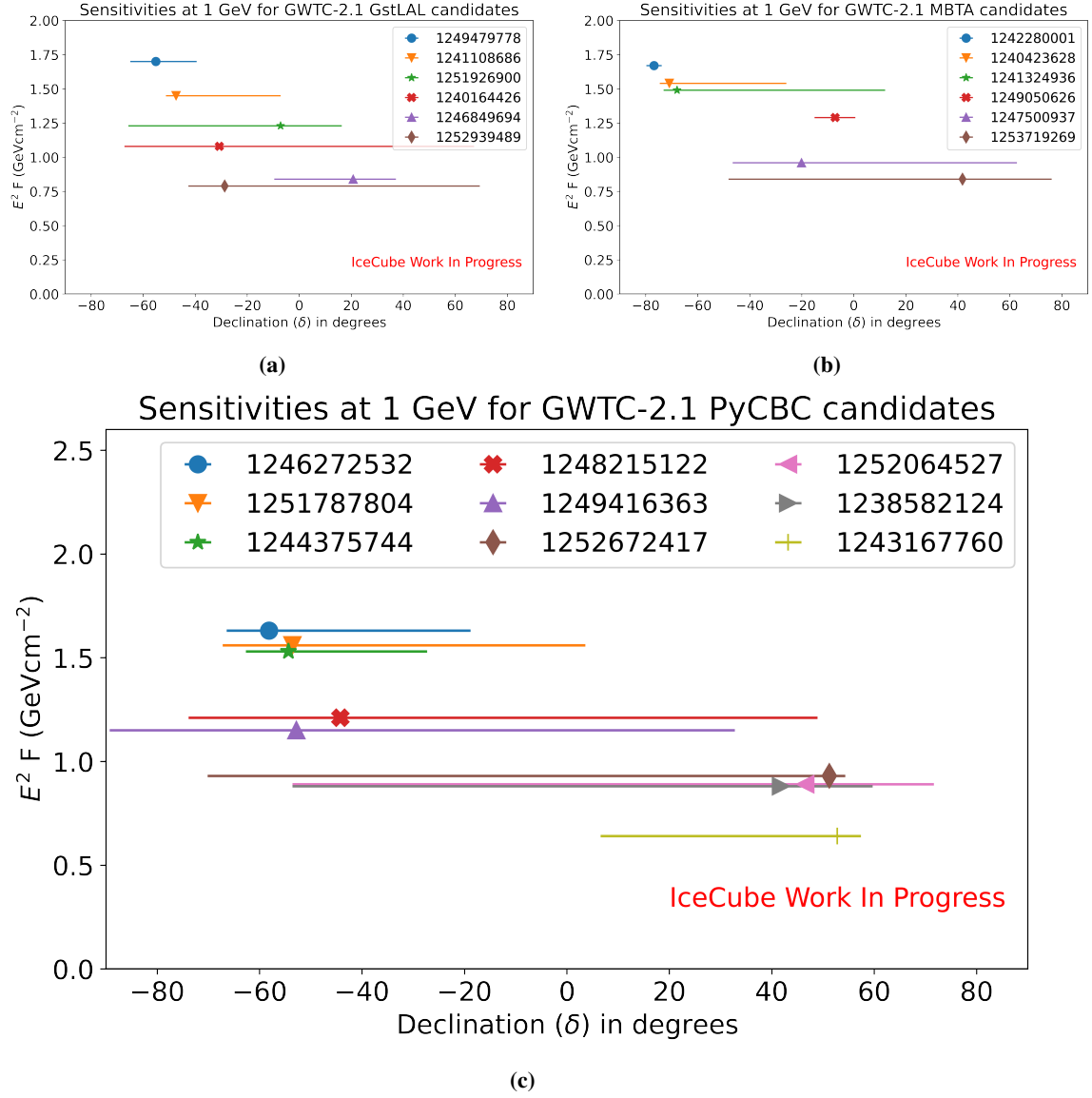
(a)

(b)

(c)

Figure 6: Declination dependence of per-flavour sensitivity flux calculated at 1 GeV for the sub-threshold candidates identified by (a) GstLAL (b) MBTA (c) PyCBC during O3a. The declination of the pixel containing with the best-fit source location has been shown by a marker.The horizontal spread across the markers covers the declination range for 50% containment area from the respective GW skymap.

different n_s values on the GW skymap to generate different TS values, and compare that with the BGTS distribution. This is also repeated for 10,000 times for each sub-threshold GW candidate. For each different n_s value, we will have a different flux recorded by our detector. We calculate for each flux level, the Passing Fraction (PF), which is the fraction of the pseudo experiments where, for neutrino injection, we have a TS value higher than the median of BGTS. The flux for which we obtain PF = 0.9, is our 90% sensitivity flux for the given dataset. In Figure 5, we show the PF curve for S1246849694 as an example.

We also study the declination dependence of per-flavour sensitivity of the sub-threshold GW

candidates. In Figure 6, we show the sensitivities of the sub-threshold candidates identified by the GstLAL, MBTA and PyCBC pipeline. From this figure, we see the general behaviour is to have better sensitivities in the Northern Hemisphere than in the Southern Hemisphere. This is a well-known feature of GRECO which was also identified in a previous analysis [8]. Also, it is notable that even the 50% containment region for some of the sub-threshold candidates is pretty large, ranging from the Northern to the Southern hemisphere. The main reason for this is worse localisation of sub-threshold candidates by the GW detectors. However, this could be significantly improved if we can identify neutrino counterparts spatially and temporally correlated to these candidates.

5. Outlook

Neutrino counterpart search for confident GW events have been conducted by IceCube over all possible energy ranges, from few GeV to O(100) GeV. In this work, we look for spatially coincident sub-TeV neutrinos with sub-threshold GW candidates, within 1000 s time window. We have completed per-flavour sensitivity studies for the GW candidates with $p_{\text{astro}} > 0.1$. Declination dependence of per-flavour sensitivity has been shown for candidates from three different pipelines - GstLAL, MBTA and PyCBC. Notably, for some sub-threshold GW candidates, the localisation is particularly worse. If identifying coincident neutrino events is possible, the GW source localisation could be significantly improved. This would not only make future follow-ups of sub-threshold GW candidates more efficient, but also help us to gather maximum information from the GW progenitors.

References

[1] **IceCube** Collaboration, R. Abbasi *et al. Astroparticle physics* **35** no. 10, (2012) 615.

[2] **IceCube** Collaboration, R. Abbasi *et al. The Astrophysical Journal* **944** no. 1, (2023) 80.

[3] **IceCube** Collaboration, J. Thwaites *et al. PoS* **ICRC2023** (these proceedings) 1484.

[4] **The LIGO Scientific and the Virgo** Collaborations, B. Abbott, *et al. Physical Review X* **9** no. 3, (2019) 031040.

[5] **The LIGO Scientific and the Virgo** Collaborations, R. Abbott, *et al. Physical Review X* **11** no. 2, (2021) 021053.

[6] **The LIGO Scientific, the Virgo and the KAGRA** Collaborations, R. Abbott, *et al. arXiv:2111.03606 (2021)* .

[7] **The LIGO Scientific and the Virgo** Collaborations, R. Abbott, *et al. arXiv:2108.01045 (2021)* .

[8] **IceCube** Collaboration, R. Abbasi *et al. arXiv:2303.15970 (2023)* .

[9] K. Cannon *et al. SoftwareX* **14** (2021) 100680.

[10] F. Aubin *et al. Classical and Quantum Gravity* **38** no. 9, (2021) 095004.

[11] S. A. Usman *et al. Classical and Quantum Gravity* **33** no. 21, (2016) 215004.

[12] A. H. Nitz *Classical and Quantum Gravity* **35** no. 3, (2018) 035016.

[13] **IceCube** Collaboration, R. Abbasi *et al. arXiv:2212.06810 (2022)* .

[14] M. Larson, J. Koskinen, A. Pizzuto, and J. Vandenbroucke *arXiv:2108.01530 (2021)* .

[15] **IceCube** Collaboration, R. Abbasi *et al. The Astrophysical Journal Letters* **946** no. 1, (2023) L26.

Full Author List: IceCube Collaboration

R. Abbasi[17], M. Ackermann[63], J. Adams[18], S. K. Agarwalla[40, 64], J. A. Aguilar[12], M. Ahlers[22], J.M. Alameddine[23], N. M. Amin[44], K. Andeen[42], G. Anton[26], C. Argüelles[14], Y. Ashida[53], S. Athanasiadou[63], S. N. Axani[44], X. Bai[50], A. Balagopal V.[40], M. Baricevic[40], S. W. Barwick[30], V. Basu[40], R. Bay[8], J. J. Beatty[20, 21], J. Becker Tjus[11, 65], J. Beise[61], C. Bellenghi[27], C. Benning[1], S. BenZvi[52], D. Berley[19], E. Bernardini[48], D. Z. Besson[36], E. Blaufuss[19], S. Blot[63], F. Bontempo[31], J. Y. Book[14], C. Boscolo Meneguolo[48], S. Böser[41], O. Botner[61], J. Böttcher[1], E. Bourbeau[22], J. Braun[40], B. Brinson[6], J. Brostean-Kaiser[63], R. T. Burley[2], R. S. Busse[43], D. Butterfield[40], M. A. Campana[49], K. Carloni[14], E. G. Carnie-Bronca[2], S. Chattopadhyay[40, 64], N. Chau[12], C. Chen[6], Z. Chen[55], D. Chirkin[40], S. Choi[56], B. A. Clark[19], L. Classen[43], A. Coleman[61], G. H. Collin[15], A. Connolly[20, 21], J. M. Conrad[15], P. Coppin[13], P. Correa[13], D. F. Cowen[59, 60], P. Dave[6], C. De Clercq[13], J. J. DeLaunay[58], D. Delgado[14], S. Deng[1], K. Deoskar[54], A. Desai[40], P. Desiati[40], K. D. de Vries[13], G. de Wasseige[37], T. DeYoung[24], A. Diaz[15], J. C. Díaz-Vélez[40], M. Dittmer[43], A. Domi[26], H. Dujmovic[40], M. A. DuVernois[40], T. Ehrhardt[41], P. Eller[27], E. Ellinger[62], S. El Mentawi[1], D. Elsässer[23], R. Engel[31, 32], H. Erpenbeck[40], J. Evans[19], P. A. Evenson[44], K. L. Fan[19], K. Fang[40], K. Farrag[16], A. R. Fazely[7], A. Fedynitch[57], N. Feigl[10], S. Fiedlschuster[26], C. Finley[54], L. Fischer[63], D. Fox[59], A. Franckowiak[11], A. Fritz[41], P. Fürst[1], J. Gallagher[39], E. Ganster[1], A. Garcia[14], L. Gerhardt[9], A. Ghadimi[58], C. Glaser[61], T. Glauch[27], T. Glüsenkamp[26, 61], N. Goehlke[32], J. G. Gonzalez[44], S. Goswami[58], D. Grant[24], S. J. Gray[19], O. Gries[1], S. Griffin[40], S. Griswold[52], K. M. Groth[22], C. Günther[1], P. Gutjahr[23], C. Haack[26], A. Hallgren[61], R. Halliday[24], L. Halve[1], F. Halzen[40], H. Hamdaoui[55], M. Ha Minh[27], K. Hanson[40], J. Hardin[15], A. A. Harnisch[24], P. Hatch[33], A. Haungs[31], K. Helbing[62], J. Hellrung[11], F. Henningsen[27], L. Heuermann[1], N. Heyer[61], S. Hickford[62], A. Hidvegi[54], C. Hill[16], G. C. Hill[2], K. D. Hoffman[19], S. Hori[40], K. Hoshina[40, 66], W. Hou[31], T. Huber[31], K. Hultqvist[54], M. Hünnefeld[23], R. Hussain[40], K. Hymon[23], S. In[56], A. Ishihara[16], M. Jacquart[40], O. Janik[1], M. Jansson[54], G. S. Japaridze[5], M. Jeong[56], M. Jin[14], B. J. P. Jones[4], D. Kang[31], W. Kang[56], X. Kang[49], A. Kappes[43], D. Kappesser[41], L. Kardum[23], T. Karg[63], M. Karl[27], A. Karle[40], U. Katz[26], M. Kauer[40], J. L. Kelley[40], A. Khatee Zathul[40], A. Kheirandish[34, 35], J. Kiryluk[55], S. R. Klein[8, 9], A. Kochocki[24], R. Koirala[44], H. Kolanoski[10], T. Kontrimas[27], L. Köpke[41], C. Kopper[26], D. J. Koskinen[22], P. Koundal[31], M. Kovacevich[49], M. Kowalski[10, 63], T. Kozynets[22], J. Krishnamoorthi[40, 64], K. Kruiswijk[37], E. Krupczak[24], A. Kumar[63], E. Kun[11], N. Kurahashi[49], N. Lad[63], C. Lagunas Gualda[63], M. Lamoureux[37], M. J. Larson[19], S. Latseva[1], F. Lauber[62], J. P. Lazar[14, 40], J. W. Lee[56], K. Leonard DeHolton[60], A. Leszczyńska[44], M. Lincetto[11], Q. R. Liu[40], M. Liubarska[25], E. Lohfink[41], C. Love[49], C. J. Lozano Mariscal[43], L. Lu[40], F. Lucarelli[28], W. Luszczak[20, 21], Y. Lyu[8, 9], J. Madsen[40], K. B. M. Mahn[24], Y. Makino[40], E. Manao[27], S. Mancina[40, 48], W. Marie Sainte[40], I. C. Mariş[12], S. Marka[46], Z. Marka[46], M. Marsee[58], I. Martinez-Soler[14], R. Maruyama[45], F. Mayhew[24], T. McElroy[25], F. McNally[38], J. V. Mead[22], K. Meagher[40], S. Mechbal[63], A. Medina[21], M. Meier[16], Y. Merckx[13], L. Merten[11], J. Micallef[24], J. Mitchell[7], T. Montaruli[28], R. W. Moore[25], Y. Morii[16], R. Morse[40], M. Moulai[40], T. Mukherjee[31], R. Naab[63], R. Nagai[16], M. Nakos[40], U. Naumann[62], J. Necker[63], A. Negi[4], M. Neumann[43], H. Niederhausen[24], M. U. Nisa[24], A. Noell[1], A. Novikov[44], S. C. Nowicki[24], A. Obertacke Pollmann[16], V. O'Dell[40], M. Oehler[31], B. Oeyen[29], A. Olivas[19], R. Ørsøe[27], J. Osborn[40], E. O'Sullivan[61], H. Pandya[44], N. Park[33], G. K. Parker[4], E. N. Paudel[44], L. Paul[42, 50], C. Pérez de los Heros[61], J. Peterson[40], S. Philippen[1], A. Pizzuto[40], M. Plum[50], A. Pontén[61], Y. Popovych[41], M. Prado Rodriguez[40], B. Pries[24], R. Procter-Murphy[19], G. T. Przybylski[9], C. Raab[37], J. Rack-Helleis[41], K. Rawlins[3], Z. Rechav[40], A. Rehman[44], P. Reichherzer[11], G. Renzi[12], E. Resconi[27], S. Reusch[63], W. Rhode[23], B. Riedel[40], A. Rifaie[1], E. J. Roberts[2], S. Robertson[8, 9], S. Rodan[56], G. Roellinghoff[56], M. Rongen[26], C. Rott[53, 56], T. Ruhe[23], L. Ruohan[27], D. Ryckbosch[29], I. Safa[14, 40], J. Saffer[32], D. Salazar-Gallegos[24], P. Sampathkumar[31], S. E. Sanchez Herrera[24], A. Sandrock[62], M. Santander[58], S. Sarkar[25], S. Sarkar[47], J. Savelberg[1], P. Savina[40], M. Schaufel[1], H. Schieler[31], S. Schindler[26], L. Schlickmann[1], B. Schlüter[43], F. Schlüter[12], N. Schmeisser[62], T. Schmidt[19], J. Schneider[26], F. G. Schröder[31, 44], L. Schumacher[26], G. Schwefer[1], S. Sclafani[19], D. Seckel[44], M. Seikh[36], S. Seunarine[51], R. Shah[49], A. Sharma[61], S. Shefali[32], N. Shimizu[16], M. Silva[40], B. Skrzypek[14], B. Smithers[4], R. Snihur[40], J. Soedingrekso[23], A. Søgaard[22], D. Soldin[32], P. Soldin[1], G. Sommani[11], C. Spannfellner[27], G. M. Spiczak[51], C. Spiering[63], M. Stamatikos[21], T. Stanev[44], T. Stezelberger[9], T. Stürwald[62], T. Stuttard[22], G. W. Sullivan[19], I. Taboada[6], S. Ter-Antonyan[7], M. Thiesmeyer[1], W. G. Thompson[14], J. Thwaites[40], S. Tilav[44], K. Tollefson[24], C. Tönnis[56], S. Toscano[12], D. Tosi[40], A. Trettin[63], C. F. Tung[6], R. Turcotte[31], J. P. Twagirayezu[24], B. Ty[40], M. A. Unland Elorrieta[43], A. K. Upadhyay[40, 64], K. Upshaw[7], N. Valtonen-Mattila[61], J. Vandenbroucke[40], N. van Eijndhoven[13], D. Vannerom[15], J. van Santen[63], J. Vara[43], J. Veitch-Michaelis[40], M. Venugopal[31], M. Vereecken[37], S. Verpoest[44], D. Veske[46], A. Vijai[19], C. Walck[54], C. Weaver[24], P. Weigel[15], A. Weindl[31], J. Weldert[60], C. Wendt[40], J. Werthebach[23], M. Weyrauch[31], N. Whitehorn[24], C. H. Wiebusch[1], N. Willey[24], D. R. Williams[58], L. Witthaus[23], A. Wolf[1], M. Wolf[27], G. Wrede[26], X. W. Xu[7], J. P. Yanez[25], E. Yildizci[40], S. Yoshida[16], R. Young[36], F. Yu[14], S. Yu[24], T. Yuan[40], Z. Zhang[55], P. Zhelnin[14], M. Zimmerman[40]

[1] III. Physikalisches Institut, RWTH Aachen University, D-52056 Aachen, Germany
[2] Department of Physics, University of Adelaide, Adelaide, 5005, Australia
[3] Dept. of Physics and Astronomy, University of Alaska Anchorage, 3211 Providence Dr., Anchorage, AK 99508, USA
[4] Dept. of Physics, University of Texas at Arlington, 502 Yates St., Science Hall Rm 108, Box 19059, Arlington, TX 76019, USA
[5] CTSPS, Clark-Atlanta University, Atlanta, GA 30314, USA
[6] School of Physics and Center for Relativistic Astrophysics, Georgia Institute of Technology, Atlanta, GA 30332, USA
[7] Dept. of Physics, Southern University, Baton Rouge, LA 70813, USA
[8] Dept. of Physics, University of California, Berkeley, CA 94720, USA
[9] Lawrence Berkeley National Laboratory, Berkeley, CA 94720, USA
[10] Institut für Physik, Humboldt-Universität zu Berlin, D-12489 Berlin, Germany
[11] Fakultät für Physik & Astronomie, Ruhr-Universität Bochum, D-44780 Bochum, Germany
[12] Université Libre de Bruxelles, Science Faculty CP230, B-1050 Brussels, Belgium

[13] Vrije Universiteit Brussel (VUB), Dienst ELEM, B-1050 Brussels, Belgium

[14] Department of Physics and Laboratory for Particle Physics and Cosmology, Harvard University, Cambridge, MA 02138, USA

[15] Dept. of Physics, Massachusetts Institute of Technology, Cambridge, MA 02139, USA

[16] Dept. of Physics and The International Center for Hadron Astrophysics, Chiba University, Chiba 263-8522, Japan

[17] Department of Physics, Loyola University Chicago, Chicago, IL 60660, USA

[18] Dept. of Physics and Astronomy, University of Canterbury, Private Bag 4800, Christchurch, New Zealand

[19] Dept. of Physics, University of Maryland, College Park, MD 20742, USA

[20] Dept. of Astronomy, Ohio State University, Columbus, OH 43210, USA

[21] Dept. of Physics and Center for Cosmology and Astro-Particle Physics, Ohio State University, Columbus, OH 43210, USA

[22] Niels Bohr Institute, University of Copenhagen, DK-2100 Copenhagen, Denmark

[23] Dept. of Physics, TU Dortmund University, D-44221 Dortmund, Germany

[24] Dept. of Physics and Astronomy, Michigan State University, East Lansing, MI 48824, USA

[25] Dept. of Physics, University of Alberta, Edmonton, Alberta, Canada T6G 2E1

[26] Erlangen Centre for Astroparticle Physics, Friedrich-Alexander-Universität Erlangen-Nürnberg, D-91058 Erlangen, Germany

[27] Technical University of Munich, TUM School of Natural Sciences, Department of Physics, D-85748 Garching bei München, Germany

[28] Département de physique nucléaire et corpusculaire, Université de Genève, CH-1211 Genève, Switzerland

[29] Dept. of Physics and Astronomy, University of Gent, B-9000 Gent, Belgium

[30] Dept. of Physics and Astronomy, University of California, Irvine, CA 92697, USA

[31] Karlsruhe Institute of Technology, Institute for Astroparticle Physics, D-76021 Karlsruhe, Germany

[32] Karlsruhe Institute of Technology, Institute of Experimental Particle Physics, D-76021 Karlsruhe, Germany

[33] Dept. of Physics, Engineering Physics, and Astronomy, Queen's University, Kingston, ON K7L 3N6, Canada

[34] Department of Physics & Astronomy, University of Nevada, Las Vegas, NV, 89154, USA

[35] Nevada Center for Astrophysics, University of Nevada, Las Vegas, NV 89154, USA

[36] Dept. of Physics and Astronomy, University of Kansas, Lawrence, KS 66045, USA

[37] Centre for Cosmology, Particle Physics and Phenomenology - CP3, Université catholique de Louvain, Louvain-la-Neuve, Belgium

[38] Department of Physics, Mercer University, Macon, GA 31207-0001, USA

[39] Dept. of Astronomy, University of Wisconsin–Madison, Madison, WI 53706, USA

[40] Dept. of Physics and Wisconsin IceCube Particle Astrophysics Center, University of Wisconsin–Madison, Madison, WI 53706, USA

[41] Institute of Physics, University of Mainz, Staudinger Weg 7, D-55099 Mainz, Germany

[42] Department of Physics, Marquette University, Milwaukee, WI, 53201, USA

[43] Institut für Kernphysik, Westfälische Wilhelms-Universität Münster, D-48149 Münster, Germany

[44] Bartol Research Institute and Dept. of Physics and Astronomy, University of Delaware, Newark, DE 19716, USA

[45] Dept. of Physics, Yale University, New Haven, CT 06520, USA

[46] Columbia Astrophysics and Nevis Laboratories, Columbia University, New York, NY 10027, USA

[47] Dept. of Physics, University of Oxford, Parks Road, Oxford OX1 3PU, United Kingdom

[48] Dipartimento di Fisica e Astronomia Galileo Galilei, Università Degli Studi di Padova, 35122 Padova PD, Italy

[49] Dept. of Physics, Drexel University, 3141 Chestnut Street, Philadelphia, PA 19104, USA

[50] Physics Department, South Dakota School of Mines and Technology, Rapid City, SD 57701, USA

[51] Dept. of Physics, University of Wisconsin, River Falls, WI 54022, USA

[52] Dept. of Physics and Astronomy, University of Rochester, Rochester, NY 14627, USA

[53] Department of Physics and Astronomy, University of Utah, Salt Lake City, UT 84112, USA

[54] Oskar Klein Centre and Dept. of Physics, Stockholm University, SE-10691 Stockholm, Sweden

[55] Dept. of Physics and Astronomy, Stony Brook University, Stony Brook, NY 11794-3800, USA

[56] Dept. of Physics, Sungkyunkwan University, Suwon 16419, Korea

[57] Institute of Physics, Academia Sinica, Taipei, 11529, Taiwan

[58] Dept. of Physics and Astronomy, University of Alabama, Tuscaloosa, AL 35487, USA

[59] Dept. of Astronomy and Astrophysics, Pennsylvania State University, University Park, PA 16802, USA

[60] Dept. of Physics, Pennsylvania State University, University Park, PA 16802, USA

[61] Dept. of Physics and Astronomy, Uppsala University, Box 516, S-75120 Uppsala, Sweden

[62] Dept. of Physics, University of Wuppertal, D-42119 Wuppertal, Germany

[63] Deutsches Elektronen-Synchrotron DESY, Platanenallee 6, 15738 Zeuthen, Germany

[64] Institute of Physics, Sachivalaya Marg, Sainik School Post, Bhubaneswar 751005, India

[65] Department of Space, Earth and Environment, Chalmers University of Technology, 412 96 Gothenburg, Sweden

[66] Earthquake Research Institute, University of Tokyo, Bunkyo, Tokyo 113-0032, Japan

Acknowledgements

PoS(ICRC2023)1504